

Clusters as Ligands. 4. Synthesis, Structure, and Characterization of the Tungsten(II)–Tungsten(III) Cluster Carboxylate



Victor Calvo-Perez,[†] Thomas P. Fehlner,^{*,†} and Arnold L. Rheingold^{*,‡}

Department of Chemistry and Biochemistry, University of Notre Dame, Notre Dame, Indiana 46556, and Department of Chemistry and Biochemistry, University of Delaware, Newark, Delaware 19716

Received August 1, 1996[⊗]

The reaction of $\text{W}_2(\text{OCCCF}_3)_4$ with $(\text{CO})_9\text{Co}_3\text{CCOOH}$ and $\text{Na}[\text{OCCCF}_3]$ in a nonpolar solvent mixture leads to the formation of the cluster of clusters $\{[\text{Na}][\text{W}_2\{\text{OCCCCo}_3(\text{CO})_9\}_2(\text{OCCCF}_3)_4(\text{THF})_2]\}_2$, **1**, in 40% yield. The structure of $\mathbf{1} \cdot 3\text{C}_6\text{H}_5\text{CH}_3$ in the solid state corresponds to a dimer of W_2 dinuclear complexes (monoclinic $P2_1/c$, $a = 15.234(6)$ Å, $b = 23.326(11)$ Å, $c = 20.658(7)$ Å, $\beta = 102.46(3)^\circ$; $V = 7,168(5)$ Å³; $Z = 4$; $R_F = 8.39\%$). Each W_2 unit is bridged by two cis cluster carboxylates, and the remaining four equatorial sites are occupied by monodentate $[\text{OCCCF}_3]^-$ ligands. The axial positions contain coordinated THF. The W_2 carboxylate is opened up ($\text{W}–\text{W}$ distance of 2.449(2) Å) so that the free ends of the $[\text{OCCCF}_3]^-$ ligands on both W_2 carboxylate units can cooperate in chelating two Na^+ ions thereby forming a dimer of W_2 complexes. A distinctive EPR spectrum with $g = 2.08$ is consistent with each W_2 carboxylate being a mixed-valent $\text{W}(\text{II})–\text{W}(\text{III})$ species. The reaction of $\text{W}_2(\text{OCCCF}_3)_4$ with $(\text{CO})_9\text{Co}_3\text{CCOOH}$ in THF in the absence of $\text{Na}[\text{OCCCF}_3]$ leads to the expected diamagnetic $\text{W}(\text{II})–\text{W}(\text{II})$ cluster carboxylate $\text{W}_2\{\text{OCCCCo}_3(\text{CO})_9\}_3(\text{OCCCF}_3)(\text{THF})_2$, **3**.

Introduction

The chemistry of $\text{W}(\text{II})$ carboxylates is markedly different from that of $\text{Mo}(\text{II})$. For example, $\text{W}(\text{II})$ is prone to oxidative addition whereas $\text{Mo}(\text{III})$ tends to reductively eliminate ligands.^{1,2} Consequently, the $\text{W}(\text{II})$ carboxylates are not prepared by the route used to synthesize $\text{Mo}_2(\text{OOCR})_4$. In fact, when this approach is applied to tungsten it leads to the formation of W -bridged oxo trimers with oxidation states in the range $\text{III}–\text{V}$.^{3–5} The reaction of $\text{W}_2\text{Cl}_4(\text{THF})_2$, formed *in situ*, with $\text{Na}[\text{OOCR}]$ is the practicable route to $\text{W}(\text{II})$ carboxylates.^{6,7} On the other hand, dimeric $\text{W}(\text{III})$ carboxylates have been prepared and characterized starting from the $\text{W}(\text{III})$ alkoxides and the corresponding carboxylic acids.⁸ Alternatively, the oxidative addition of an acid such as HCl to a $\text{W}(\text{II})$ dimer can be carried out.³

We have shown that the cluster ligand $[\text{OCCCCo}_3(\text{CO})_9]^-$ readily replaces the acetate ligands in $\text{Mo}_2(\text{OOCCH}_3)_4$ to yield $\text{Mo}_2\{\text{OOC}–\text{CCo}_3(\text{CO})_9\}_{4-n}(\text{OOCCH}_3)_n$, $n = 0$ and 1, in an exchange reaction with the free cluster acid.⁹ As we wished to compare the spectroscopic properties of the molybdenum cluster of clusters with its $\text{Cr}(\text{II})$ and $\text{W}(\text{II})$ analogs, we explored the direct reaction of $\text{W}_2(\text{OCCCF}_3)_4$ with $(\text{CO})_9\text{Co}_3\text{CCOOH}$. Al-

though the desired compound was eventually forthcoming,¹⁰ our initial attempts led to the isolation of a compound intermediate in composition between that of the initial $\text{W}(\text{II})$ trifluoroacetate dimer and the desired product. In the following we describe this unusual compound and provide a convenient synthesis.

Experimental Section

Materials and Methods. Due to the air sensitivity of the $\text{W}(\text{II})$ carboxylates, all compounds were handled under argon in a Schlenk line or under nitrogen in a drybox. Infrared spectra were measured on a Nicolet 205 FTIR spectrometer. The samples were ground with dry KBr and loaded in the IR press in a drybox and quickly measured outside the box. EPR spectra were recorded on a Bruker 1600 spectrometer working in the X-band and equipped with an Oxford variable-temperature controller. Typically 5–50 mg of a crystalline sample in a quartz capillary tube sealed under vacuum was examined. Electronic spectra were measured under argon in supracells with a glass stopcock in a Perkin-Elmer spectrophotometer (Model 6 or 19). $(\text{CO})_9\text{Co}_3\text{CCOOH}$ ^{11–13} and $\text{W}_2(\text{OCCCF}_3)_4$ ⁷ were prepared by literature methods. Elemental analyses were by MHW Laboratories. However, metal analyses for compounds that easily lost solvent were carried out in house using a Perkin-Elmer ICP spectrometer and standard techniques.¹⁴

Preparation of Compounds. $\{[\text{Na}][\text{W}_2\{\text{OCCCCo}_3(\text{CO})_9\}_2(\text{OCCCF}_3)_4(\text{THF})_2]\}_2 \cdot 3\text{C}_6\text{H}_5\text{CH}_3$, $\mathbf{1} \cdot 3\text{C}_6\text{H}_5\text{CH}_3$. To 0.70 g (0.85 mmol) of $\text{W}_2(\text{OCCCF}_3)_4$ and 115 mg (0.85 mmol) of $\text{Na}[\text{OCCCF}_3]$ in a 150 mL Schlenk tube equipped with two stopcocks and a magnetic stirring bar was added 35 mL of toluene to dissolve the solids. In a separate Schlenk tube, 850 mg (1.75 mmol) of $(\text{CO})_9\text{Co}_3\text{CCOOH}$ was dissolved in 7 mL of freshly distilled THF. The cluster ligand solution was transferred by cannula to the tungsten(II) trifluoroacetate solution and stirred at room temperature. The immediate green color slowly turned to blue. After 60 min the solvent and any CF_3COOH was removed under vacuum with the last being removed at 45 °C leaving

[†] University of Notre Dame.

[‡] University of Delaware.

[⊗] Abstract published in *Advance ACS Abstracts*, November 1, 1996.

- (1) Chisholm, M. H. *Angew. Chem., Int. Ed. Engl.* **1986**, *25*, 21.
- (2) Chisholm, M. H.; Chiu, H. T.; Huffman, J. C. *Polyhedron* **1984**, *3*, 759.
- (3) Cotton, F. A.; Mott, G. N. *J. Am. Chem. Soc.* **1982**, *104*, 5978.
- (4) Bino, A.; Cotton, F. A.; Dori, Z.; Shaia-Gottlieb, M.; Kapon, M. *Inorg. Chem.* **1988**, *27*, 3592.
- (5) Ardon, M.; Cotton, F. A.; Dori, Z.; Fang, A.; Kapon, M.; Reisner, G. M.; Shaia, M. *J. Am. Chem. Soc.* **1982**, *104*, 5394.
- (6) Santure, D. J.; McLaughlin, K. W.; Huffman, J. C.; Sattelberger, A. P. *Inorg. Chem.* **1983**, *22*, 1877.
- (7) Santure, D. J.; Sattelberger, A. P. *Inorg. Synth.* **1989**, *26*, 219.
- (8) Chisholm, M. H.; Heppert, J. A.; Hoffman, D. M.; Huffman, J. C. *Inorg. Chem.* **1985**, *24*, 3214.
- (9) Cen, W.; Lindenfeld, P.; Fehlner, T. P. *J. Am. Chem. Soc.* **1992**, *114*, 5451.

(10) Fehlner, T. P.; Calvo-Perez, V.; Cen, W. **1993**, *66*, 29.

(11) Nivert, C. L.; Williams, G. H.; Seyferth, D. *Inorg. Synth.* **1980**, *20*, 234.

(12) Seyferth, D. *Adv. Organomet. Chem.* **1976**, *14*, 97.

(13) Cen, W.; Haller, K. J.; Fehlner, T. P. *Inorg. Chem.* **1993**, *32*, 995.

(14) Montaser, A.; Fassel, V. A. *Anal. Chem.* **1978**, *48*, 1490.

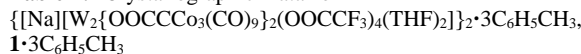
a black solid. The black solid was extracted with 50 mL of toluene from which was isolated 20 mg of green crystalline solid (1.2% of **3**; see below).

The remaining black-blue solid (600 mg), with an IR spectrum distinctly different from that of **3**, was redissolved in 10 mL of THF, filtered, and concentrated to 5 mL. After dilution with 5 mL of freshly distilled toluene, the blue solution was layered with 15 mL of pentanes under Ar. After 2 days in the refrigerator (10 °C) and 3 days in the freezer (−20 °C), 500 mg of black-blue prismatic crystals was isolated. A second crop of 120 mg gave a total yield of 39% based on $W_2(OOCCF_3)_4$. This material was recrystallized from toluene layered with hexanes in similar manner to yield 300 mg of crystals suitable for X-ray diffraction. Anal. Obsd for dried sample: C, 21.26; H, 0.68; F, 9.44. Calcd for $C_{34}H_8F_{12}Co_6Na_1W_2O_{31}$: C, 21.67; H, 0.43; F, 12.10 (corresponding to $Na[W_2\{OOCCO_3(CO)_9\}_2(OOCCF_3)_4(THF)]$). Obsd for freshly prepared sample: Na, 1.05; W, 16.68; Co, 16.42 (Co/W mole/ratio 3.07). Calcd for $C_{48.5}H_{28}F_{12}Co_6W_2NaO_{32}$: Na, 1.10; W, 17.55; Co, 16.88 (corresponding to $Na[W_2\{OOCCO_3(CO)_9\}_2(OOCCF_3)_4-Na(THF)_2]^{3/2}C_6H_5CH_3$). EPR (X-band, toluene, 25 °C): $g = 2.06$, Δ peak-to-peak = 300 G. (X-band, 5 mg of crystalline solid, 25 °C): $g = 2.08$, Δ peak-to-peak = 283 G. FT-IR (KBr, cm^{-1}): 2106 (w), 2061 (s), 1733 (m), 1427 (m), 1384 (m), 1194 (m), 1154 (sh), 1110 (w), 872–850 (w), 770 (w), 723 (w), 553 (w), 500 (w), 416 (w). Vis (toluene): 690 (ϵ 13 200 $cm^{-1} M^{-1}$), 625 nm (shoulder). Vis (hexanes): 728, 625 nm (shoulder).

$Na[W_2\{OOCCO_3(CO)_9\}(OOCCF_3)_5]$, **2**. To 0.71 g (0.87 mmol) of $W_2(OOCCF_3)_4$ and 0.115 g (0.85 mmol) of $Na(OOCCF_3)$ in 21 mL of toluene at 35 °C under argon was added 0.80 g (1.65 mmol) of $Co_3(CO)_9CCOOH$ dissolved in 7 mL of ethyl ether. The solution turned green-blue, but after 15 min it was deep blue. After 2 h the solvents were removed under vacuum, and the black solid was dried for 10 min at 40 °C. The solid was then dispersed in 50 mL of warm toluene, and the blue toluene extract was filtered over activated silica gel. After removal of half the solvent under vacuum and layering with hexanes, 0.62 g (45%) of well-shaped crystals of **2** formed after 2 days at 10 °C and 10 days at −20 °C. Anal. Found: 22.97, C; 1.07, H; 15.30, F; 1.41, Na; 23.27, W; 10.36, Co. Calcd for $C_{27}H_{20}F_{15}Co_3Na_1W_2O_{23}$: 20.72, C; 1.29, H; 18.21, F; 1.47, Na; 23.50, W; 11.30, Co (corresponding to $Na[W_2\{OOCCO_3(CO)_9\}(OOCCF_3)_5] \cdot 2Et_2O$). EPR (X-band, 5 mg of crystalline solid, 23 °C): $g = 2.23$, Δ peak-to-peak = 550 G. FT-IR (KBr, cm^{-1}): 2989 (w), 2910 (w), 2110 (m), 2063 (s), 2049 (s), 1742–1727 (s), 1689 (sh), 1600 (w), 1432–1424 (m), 1193 (vs), 1152 (s), 1021 (w), 850 (m), 784–772 (w), 734–722 (m), 623 (w), 517 (m), 500 (m). Vis (toluene): 606 (ϵ 3822 $cm^{-1} M^{-1}$), 300 nm (ϵ 8842 $cm^{-1} M^{-1}$). The X-ray diffraction study was not successful.

$W_2\{OOCCO_3(CO)_9\}_3(OOCCF_3)(THF)_2$, **3**. A 0.25 g (0.30 mmol) amount of $W_2(OOCCF_3)_4$ was dissolved in 10 mL of THF under argon in a Schlenk tube containing a magnetic stirring bar. Then 1005 mg (2.068 mmol) of $(CO)_9Co_3CCOOH$ in 20 mL of THF was added and the mixture allowed to react in the dark¹⁵ at room temperature. After about 15 min, the solution turned from purple-brown to deep green but the reaction was continued for 4 h. The solvent and volatile CF_3COOH were removed under vacuum and the solids extracted with 30 mL of freshly distilled toluene using an ultrasonic cleaning bath to help disperse the solids. The suspension was filtered under argon on a fine Schlenk filter containing 0.5 g of activated silica gel (Baker) and then concentrated to 20 mL. Crystallization at 10 °C for 2 days yielded 0.40 g (63%) of air-sensitive green crystals.

The formation of **3** also resulted from the metathesis of $W_2(CF_3COO)_4$ with $[C_{10}H_6(NMe_2)_2H][OOC-CCO_3(CO)_9]$, prepared *in situ* by reaction of $Co_3(CO)_9CCOOH$ with 1,8- $C_{10}H_6(NMe_2)_2$ (proton sponge) in the same solvent and used immediately. The green needlelike crystals obtained gave the same IR spectrum as those isolated from the exchange of $W_2(CF_3COO)_4$ with the cluster acid. In addition, **3** could be prepared from an unusual source of the cluster ligand. Two equivalents of $[Co_4O\{O_2CCCO_3(CO)_9\}_6]$, which is known to dissociate in THF,¹³ were reacted with 1 equiv of $W_2(O_2CCF_3)_4(THF)_2$ in an ether–THF mixture (5:1) in the manner of the reaction with $HOOCCO_3(CO)_9$ itself. The formation of a green solution containing $W_2\{O_2-$

Table 1. Crystallographic Data for

fw/formula	2065.0/ $C_{44}H_{28}Co_6F_{12}NaW_2O_{33.5}$
color, dimens	black, $0.34 \times 0.34 \times 0.38$ mm
temp	228(2) K
space group	monoclinic, $P2_1/c$
<i>a</i>	15.234(6) Å
<i>b</i>	23.326(11) Å
<i>c</i>	20.658(7) Å
β	102.46(3)°
<i>V</i>	7168(5) Å ³
<i>Z</i>	4
<i>D</i> (calcd)	1.941 g/cm ³
μ	4.668 mm ^{−1}
radiation (λ)	Mo K α (0.71073 Å)
θ range	2.02–23.00°
R_F , R_{wF} ^a	0.0839, 0.1765
no. indep reflections	9943
no. variables	722
$\Delta(\rho)$	1.822, −1.372 e Å ^{−3}
diffractometer	Siemens R3m/V

$$^a R_F = \sum(\Delta/\Sigma(F_o)), R_{wF} = \sum(\Delta w^{1/2})/\Sigma(F_o w^{1/2}), \text{ where } \Delta = |F_o - F_c|.$$

Table 2. Selected Distances (Å) and Angles (deg) for $1 \cdot C_6H_5CH_3$

W(1)–O(1)	2.022(14)	O(9)–Na(1)	2.42(2)
W(1)–O(3)	2.053(13)	O(10)–Na(1)	2.22(3)
W(1)–O(5)	2.093(14)	O(11)–Na(1)	2.26(2)
W(1)–O(6)	2.05(2)	O(12)–Na(1)	2.40(3)
W(1)–O(13)	2.22(2)	F(3')–Na(1)	2.68(2)
W(1)–O(14)	2.249(14)	O(9')–Na(1)	2.38(2)
W(1)–W(2)	2.449(2)	Na \cdots Na'	3.60(2) Å
O(5)–W(1)–W(2)	112.5(4)	O(7)–W(1)–W(2)	113.9(4)
O(6)–W(1)–W(2)	115.6(5)	O(8)–W(1)–W(2)	112.0(15)

$CCC_3(CO)_9\}_3(O_2CCF_3)(THF)_2$ by IR indicated that an effective metathesis reaction had taken place. Anal. Found: 25.57, Co; 17.92, W. Calcd for $C_{43}H_{16}F_3Co_9W_2O_{37}$: 25.50, Co; 17.68, W (corresponding to freshly prepared crystals of $W_2\{OOCCO_3(CO)_9\}_3(OOCCF_3)(THF)_2$). Vis (toluene, λ): 804 (ϵ 34 000 $M^{-1} cm^{-1}$), 600 (ϵ 3500 $M^{-1} cm^{-1}$), 300 nm (ϵ 35 000 $M^{-1} cm^{-1}$). EPR (crystals, X-band, 100 mW): silent. FT-IR (KBr, cm^{-1}): 2102 (m), 2065 (s), 2044 (s), 1571 (w), 1557 (sh), 1419 (w), 1384 (w), 1330 (vw), 1209 (w), 1189 (m), 1159 (w), 750 (m), 732 (m), 734 (w), 722 (w), 555 (m), 498 (m), 465 (w). FT-IR (toluene, cm^{-1}): 2100 (m), 2067 (s), 2041 (s), 1602 (m).

Crystallographic Studies. $1 \cdot 3C_6H_5CH_3$. Black blue crystals were sealed in thin-walled capillaries due to the sensitivity of this compound to air. All samples of **1** diffracted broadly, as would be expected from a loosely bound multicomponent lattice architecture. Photographic evidence revealed that the best specimen was of adequate quality to attempt a data collection and that the Laue symmetry was $2/m$. The space group was uniquely determined from systematic absences. Data were collected slowly to the upper 2θ limit of availability. Semi-empirical corrections for absorption were applied to the data. The W atoms were located from a Patterson projection. The remainder of the non-hydrogen atoms were located from subsequent difference maps. All atoms with $Z > 6$ and C atoms 1–12 were anisotropically refined. Hydrogen atoms were idealized. All computations used SHELXTL 5.1 software.¹⁶ The crystallographic data for **1** are given in Table 1 with selected distances and angles in Table 2.

3. A data set was collected, and two W atoms, which were separated by 2.18 Å and surrounded by four oxygen atoms each, were located in the difference map. However, further refinement was discontinued because of a twinning problem.

Molecular Orbital Calculations. Fenske–Hall molecular orbital calculations^{17,18} were carried out on $Na[W_2(\mu-OOCH)_2(OOCH)_4(H_2O)_2]$ as a model for **1** (the H_2O ligands are axially coordinated) to investigate the role of axial ligand geometry on the W–W bonding. The geometry

(15) Matonic, J. H.; Chen, S.-J.; Perlepes, S. P.; Dumbar, K. R.; Christou, G. *J. Am. Chem. Soc.* **1991**, *113*, 8169.

(16) Sheldrick, G. Siemens XRD, Madison, WI.

(17) Hall, M. B.; Fenske, R. F. *Inorg. Chem.* **1972**, *11*, 768.

(18) Fenske, R. F. *Pure Appl. Chem.* **1988**, *60*, 1153.

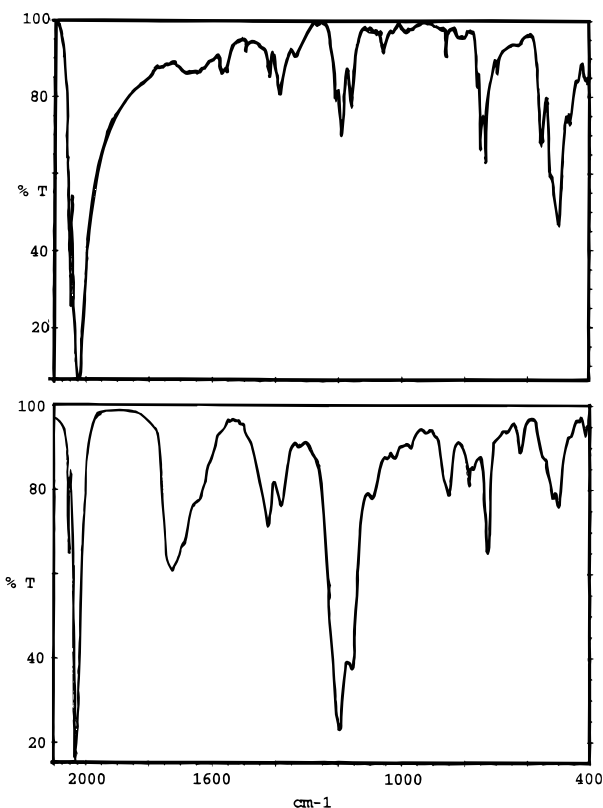
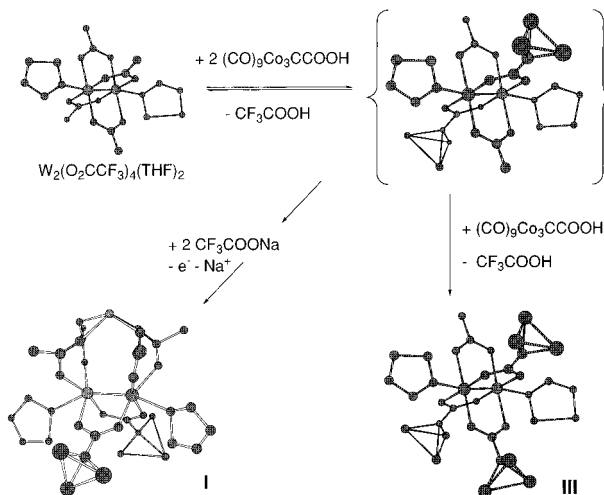


Figure 1. IR spectra of **1** (bottom) and **3** (top) in the solid state.

Scheme 1



of **1** was used, and calculations were performed with axial ligands as observed, axial ligands with O–W–W angles of 180°, and with no axial ligands at all. For reference a calculation on $[W_2(\mu\text{-OOCCH}_3)_4(\text{H}_2\text{O})_2]$ with a shorter W–W distance (2.20 vs 2.44 Å) and W centers with idealized O_h symmetry was carried out.

Results

Infrared Spectra. A comparison of the spectra of the crystalline solids is informative (Figure 1).¹⁹ The antisymmetric and symmetric carboxylate modes of the $[\text{CF}_3\text{COO}]^-$ and cluster ligands of **3** at 1571, 1419, 1384, and 1330 cm^{-1} are similar to those observed at 1518, 1439, 1366, and 1323 cm^{-1} for $\text{Mo}_2\{\text{O}(\text{O}(\text{C}(\text{O})_9\text{C}(\text{O})_9)_3)(\text{O}(\text{O}(\text{C}(\text{H}_3)_3)_3)\}$.⁹ This suggests that **3** has a similar coordination geometry (Scheme 1). The spectrum of

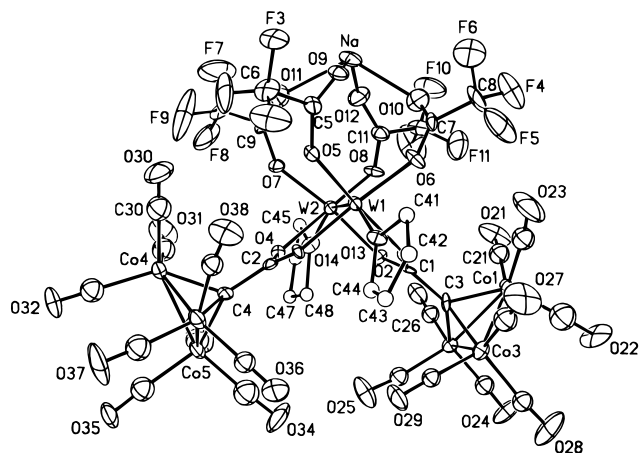


Figure 2. Molecular structure of $\{[\text{Na}][\text{W}_2\{\text{O}(\text{O}(\text{C}(\text{O})_9\text{C}(\text{O})_9)_2(\text{OOCCF}_3)_4(\text{THF})_2)\}]_2 \cdot 3\text{C}_6\text{H}_5\text{CH}_3 \cdot 1 \cdot 3\text{C}_6\text{H}_5\text{CH}_3$, showing one of the two equivalent W_2 units, i.e., $[\text{Na}][\text{W}_2\{\text{O}(\text{O}(\text{C}(\text{O})_9\text{C}(\text{O})_9)_2(\text{OOCCF}_3)_4(\text{THF})_2)\}]$.

1 in the same region has two striking differences. The medium-intensity bands at 1733 and 1384 cm^{-1} are consistent with monodentate $[\text{CF}_3\text{COO}]^-$ ligands as the difference between the symmetric and antisymmetric modes is expected to be considerably larger for this type of coordination. In addition, the intensity of the cluster carbonyl band relative to the band at $\approx 1200 \text{ cm}^{-1}$, which is associated with the CF_3 group, is much lower for **1** relative to **3**.

Solid-State Structure. $1 \cdot 3\text{C}_6\text{H}_5\text{CH}_3$ consists of two equivalent W_2 units, one of which, $[\text{Na}][\text{W}_2\{\text{O}(\text{O}(\text{C}(\text{O})_9\text{C}(\text{O})_9)_2(\text{OOCCF}_3)_4(\text{THF})_2)\}]$, is shown in Figure 2. Each W_2 unit has two W centers separated by 2.449(2) Å and two axially coordinated THF molecules ($\text{O}(14)\text{-W}(1) = 2.249(14)$ Å) bent off axis ($\text{O}(14)\text{-W}(1)\text{-W}(2) = 152.9(4)^\circ$). Each W_2 unit is bridged by two $[\text{Co}_3(\text{CO})_9\text{CCOO}]^-$ cluster ligands in cis positions with an angle of $96.9(5)^\circ$ between the two carboxylate planes. In addition each W_2 unit exhibits four monodentate $[\text{OOCCF}_3]^-$ ligands which are bent away from the W–W axis ($\text{O}(5)\text{-W}(1)\text{-W}(2)$ angle = $112.5(4)^\circ$). These two ligand arrangements are consistent with the IR data. Each W atom lies at the base of a square pyramid of oxygen atoms consisting of four basal oxygen atoms from two $[\text{OOCCF}_3]^-$ and two $[\text{Co}_3(\text{CO})_9\text{CCOO}]^-$ ligands and one apical oxygen atom from a THF molecule. The basal square planes of oxygen atoms are not coplanar, and the angle between the pseudo C_4 axes is 156° . The four trifluoroacetate groups from the W_2 unit chelate a Na cation (average $\text{Na}\text{-O} = 2.38(2)$ Å) and provide the interconnection between the two W_2 units of **1**.

This interconnection consists of Na–carboxylate oxygen and Na–trifluoromethyl fluorine interactions, and the dimer has a center of inversion that lies between the two sodium ions. As illustrated in Figure 3, each Na has six nearest neighbors consisting of four oxygen atoms from the trifluoroacetates of one W_2 unit together with a F and a O belonging to the adjacent W_2 unit. Interaction of a Na ion with fluorine is known,²⁰ and in **1** the Na–F distance of 2.68(2) Å is a little longer than that in CFH_2COONa (2.56(2) Å).²¹ As the entire species has no charge, either there are two protons in the structure that are unobserved or two of the four tungsten atoms have been oxidized to W(III) during the synthetic procedure.

Other Spectroscopic Data. Clusters **1** and **2** exhibit intense EPR signals (Figure 4) whereas **3** does not. The observed resonances are discussed below relative to known examples;

(19) Mehrotra, R. C.; Bohra, R. *Metal Carboxylates*; Academic Press: New York, 1983; p 396.

(20) Kulawiec, R. J.; Crabtree, R. H. *Coord. Chem. Rev.* **1990**, *90*, 89.

(21) Vedavathi, V. M.; Vijayan, K. *Acta Crystallogr.* **1977**, *B33*, 946.

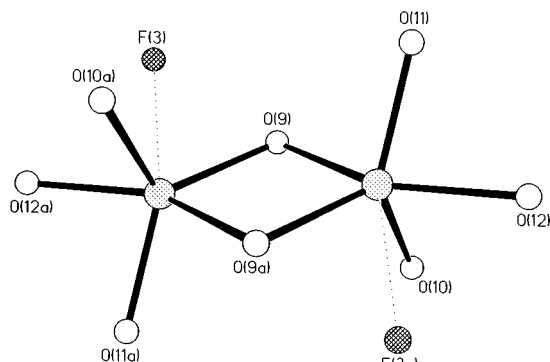


Figure 3. Coordination environment of the Na centers of $1 \cdot 3\text{C}_6\text{H}_5\text{-CH}_3$.

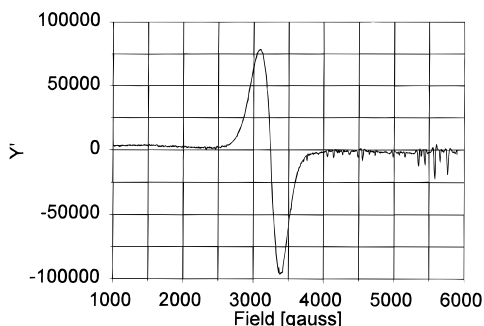


Figure 4. X-band EPR spectrum of **1** at 294 K and 9.46 GHz, 100 mW power, modulation amplitude and frequency of 5 G and 100 kHz, respectively, and gain of 10^4 .

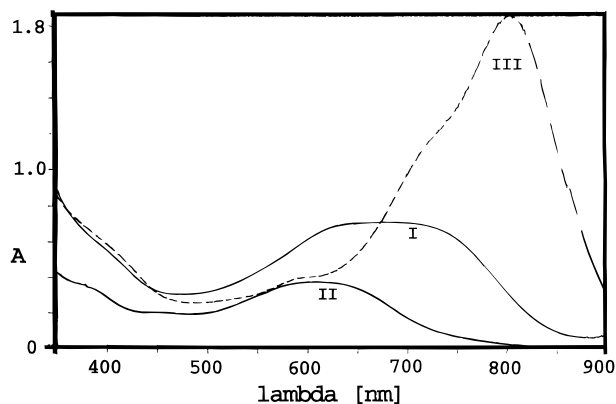


Figure 5. Visible/near-IR absorption spectra of **1–3** (I–III, respectively) in toluene solution.

however, this observation demonstrates that oxidation did take place and the observed spectrum is consistent with a mixed W(II)–W(III) core in each W_2 unit. Thus, it is unlikely that any protons on, for example, the trifluoroacetates are present.

Clusters **1–3** have absorptions in the visible–near IR (Figure 5), and the magnitudes of the extinction coefficients correspond to allowed transitions. The absorptions of **1** and **2** appear at significantly higher energy than that of **3**. Again, this suggests a difference in the oxidation states of the tungsten cores. All solutions were also carefully examined at longer wavelengths (2000 nm), but no band that could be attributed to intervalence electron transfer was observed. The band maxima of the visible spectra of these clusters are somewhat sensitive to the nature of the solvent consistent with allowed charge transfer transitions.

Discussion

Origin of **1 and **2**.** The reaction of $\text{W}_2(\text{OOCF}_3)_4$ with $(\text{CO})_9\text{Co}_3\text{CCOOH}$ in the presence of $\text{Na}[\text{OOCF}_3]$ leads to the formation of either **1** or **2** depending on exact conditions

(Scheme 1). In the absence of $\text{Na}[\text{OOCF}_3]$ and when the reaction is carried out in THF, only the expected product, **3**, is produced. The color changes observed during the reaction strongly suggest that **3** or, more precisely, $\text{W}_2\{\text{OOC}(\text{CO})_9\}_n(\text{OOCF}_3)_{4-n}$, $n = 1–3$, is initially produced in all three cases, and in fact, a small amount of **3** can be isolated from the reaction in which **1** is the major product. The formation of **1** from **3** formally requires oxidation of the W_2 complex, loss of one $[\text{OOC}(\text{CO})_9]^-$ ligand, and coordination of an additional three $[\text{OOCF}_3]^-$ ligands.

The oxidation of tungsten in the presence of carboxylic acids is well-known albeit not well understood.⁵ However, it is unlikely that the CF_3COOH generated during the exchange or the acid functional group on the cluster is the oxidizing agent. The cluster ligand exchange proceeds uneventfully to **3** in the absence of $[\text{CF}_3\text{COO}]^-$. With the tricobalt cluster substituted acid, the oxidation takes place under mild conditions and no $\text{W}_3\text{O}_2(\text{OOCR})_6(\text{OR}')_3$, which is commonly observed during the reaction of $\text{W}(\text{CO})_6$ with acetic acid,³ is observed. The cluster ligand is a potential electron acceptor which might form a coordinated or uncoordinated tricobalt cluster radical anion.^{22,23} However, this is also judged unlikely as the half wave potential for the reduction of $\text{Co}_3(\text{CO})_9\text{CCH}_3$ much more negative than that for $\text{W}_2(\text{O}_2\text{CBu})_4$.²⁴ On the other hand, the tricobalt cluster is prone to decomposition into Co^{2+} , $[\text{Co}(\text{CO})_4]^-$, organic fragments, and possibly other species.^{25–27} Consequently, it is possible that one of these species or their precursors, e.g., the ubiquitous $\text{Co}(\text{CO})_4$ radical, acts as the one electron oxidizing agent. This would be consistent with the observation that these steps take place on a longer time scale than the formation of **3**. Photochemical conversion of **3** to **1** or **2** is also possible. Although the synthetic work was carried out at reduced light levels, we cannot rule out this possibility. Finally, as already noted, the solvent also plays a role but one which is unclear.

Metrics of the W–W Bond in **1.** The meaning of the metal–metal distances in these multiply bonded systems has been extensively discussed.²⁸ A number of studies are pertinent to this work. The product of oxidative addition of HCl across the WW bond has a W–W distance of 2.423 Å with two W(III) octahedral centers sharing one edge.³ A ditungsten d^2-d^2 system is formally double bonded and displays a W–W distance of 2.481 Å.²⁹ A mixed-valence W(III)–W(IV) complex with two facial octahedral tungsten centers triply bridged by Se centers shows a W–W distance 2.5641(8) Å.³⁰ This radical species is considered to be doubly bonded. Although d^3-d^3 ditungsten systems with W–W distances in the range 2.29–2.33 Å are considered triply bonded, e.g., $\text{W}_2(\text{OOCBu})_6$,⁸ there are examples that exhibit longer W–W distances, e.g., 2.421 Å in $\text{W}_2(\text{OBU})_4(\text{OTf})_2(\text{PME}_3)_4$ which has no bridging ligands.³¹ On the basis of these reference compounds, the W–W distance

- (22) Lindsay, P. N.; Peake, B. M.; Robinson, B. H.; Simpson, J.; Honrath, U.; Vahrenkamp, H.; Bond, A. M. *Organometallics* **1984**, *3*, 413.
- (23) Hinkelmann, K.; Heinze, J.; Schacht, H.-T.; Field, J. S.; Vahrenkamp, H. *J. Am. Chem. Soc.* **1989**, *111*, 5078.
- (24) Cayton, R. H.; Chisholm, M. H.; Huffman, J. C.; Lobkovsky, E. B. *J. Am. Chem. Soc.* **1991**, *113*, 8709.
- (25) Cen, W.; Haller, K. J.; Fehlner, T. P. *Inorg. Chem.* **1991**, *30*, 3120.
- (26) Cen, W.; Haller, K. J.; Fehlner, T. P. *Organometallics* **1992**, *11*, 3499.
- (27) Albanesi, G.; Gavezzotti, E. *Lincei-Rend. Sc. Fis. Mat. Nat.* **1966**, *41*, 497.
- (28) Cotton, F. A.; Walton, R. A. *Multiple Bonds between Metal Atoms*, 2nd ed.; Oxford University Press: New York, 1993.
- (29) Anderson, L. B.; Cotton, F. A.; DeMarco, D.; Fang, A.; Iisley, W. H.; Kolthammer, B. W. S.; Walton, R. A. *J. Am. Chem. Soc.* **1981**, *103*, 5078.
- (30) Ball, J. M.; Boorman, P. M.; Fait, J. F.; Kraatz, H.-B.; Richardson, J. F.; Collison, D.; Mabbs, F. E. *Inorg. Chem.* **1990**, *29*, 3290.
- (31) Chisholm, M. H.; Cramer, K. S.; Martin, J. D.; Huffman, J. C.; Lobkovsky, E. B.; Streib, W. E. *Inorg. Chem.* **1992**, *31*, 4469.

of **1** (2.449(2) Å) places its bond order between a double (2.5 Å) and a triple bond (2.3 Å). This conclusion ignores any steric interactions between the four [CF₃COO]⁻ groups and the THF molecules. In any case, the metal–metal bond in **1** is not a quadruple bond.

EPR. Powders of both **1** ($g_{\text{iso}} = 2.08$) and **2** display broad, intense EPR signals at room temperature consistent with an oxidized W₂ center (Figure 4). There are a few known examples of paramagnetic W₂ compounds in the literature (WMo(OOCBu^t)₄I,³² W₂(OOCBu^t)₄I,³³ CpW(CO)₂³⁴), but a W(III)–W(IV) system constitutes a useful example to compare with **1**.^{30,35} The EPR signals of **1** and **2** resemble that of [W₂(Cl)(SPh)₂Cl₆]²⁻³⁵ ($g_1 = 2.311$, $g_2 = 1.893$, $g_3 = 1.747$, at RT; $\Delta p p \sim 100$ G). With a W₂ coordination geometry of two confacial octahedrons, a d³/d² electron configuration, and C_{2v} symmetry, this compound is a reasonable model for **1**. As the spin–orbit coupling reported for W(III) is smaller than that of W(IV) ($\zeta_{\text{W(III)}} \sim 600$ cm⁻¹, $\zeta_{\text{W(IV)}} = 1050$ cm⁻¹)³⁶ the g value observed for **1** is closer to that of the free electron as expected if similar ligand field strengths are assumed.

Visible/Near-IR Absorption. The strong electronic absorption bands observed in these compounds (Figure 5) originate in allowed transitions which we suggest are metal to ligand charge transfer transitions (MLCT) involving a ligand substituted with a metal cluster. We have argued previously in the case of M₂{OCCCCO₃(CO)₉}_n{OCCX₃}_{4-n}, M = Cr, Mo, and W,¹⁰ that the correlation of absorption maxima with the ionization energy of the δ bonding electrons connect them with transitions from a metal–metal bonding orbital to an empty substituent cluster metal–metal antibonding orbital (δ to σ^*). W(II) arenecarboxylates also show strong absorptions in the visible which have been characterized as MLCT.³⁷ The same is true of W(II) ordered assemblies²⁴ and tungsten halides.³⁸ With this assignment, the higher energy of the MLCT transitions in **1** and **2** vs **3** can be associated with the higher oxidation state of the W₂ core in **1** and **2** leading to a greater stability of the W–W bonding orbitals and, hence, a larger energy gap. In **1** the two cluster ligands are conjugated via the carboxylate functionalities and the W–W bonding manifold leading to greater delocalization than in **2** and a lower energy absorption maximum as observed. However, additional transitions are expected in the oxidized W₂ clusters and the observed bands do appear to be complex ones.

Nature of the W–W Bond in 1. For compound **1** the observed geometry suggests that the reduction in bond order may be a consequence of three factors. First, one of the W–W bonding orbitals will only be half-occupied and the formal bond order cannot be higher than 3.5. Second, the coordination spheres of each W atom defined by oxygen atoms can be viewed as distorted square pyramidal with C₄ axes that meet at an angle of 156° (Figure 6). One expects this to reduce the d_{z²} overlap relative to W₂(OOCF₃)₄. Third, the contribution of the d_{z²} orbitals to M–M bonding should be further reduced by the presence of the axial ligands. In fact, a $\pi^4\delta^2$ bonding scheme has been proposed previously for a W–W compound in which

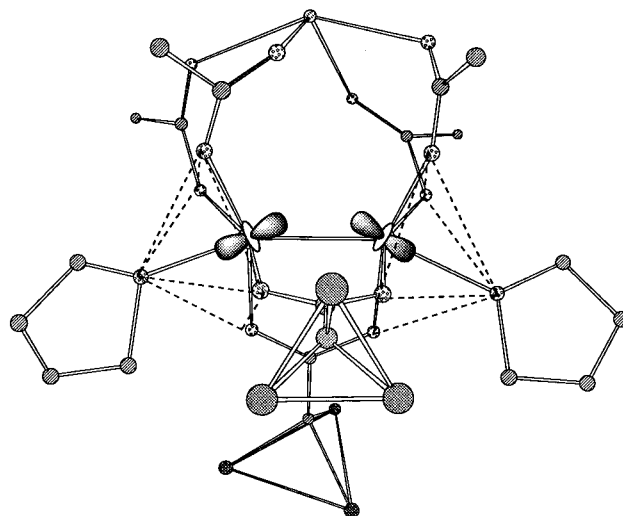


Figure 6. Representation of **1** showing the coordination environment of the W atoms and the unfavorable orientation of the W d_{z²} orbitals.

the metal is coordinated in the axial positions by alkyl groups,^{1,39} and it has been proposed that axial ligation is avoided in general because such bonding competes with the M–M σ bonding.⁸ Hence, a bond order between 2.5 and 3.5, consistent with the observed W–W distance, appears reasonable.

To test this hypothesis further an approximate MO analysis was carried out. Of course, such an MO analysis implicitly assumes delocalized oxidation states which is a situation that may well not obtain.⁴⁰ For reference [W₂(μ -OOCH)₄](H₂O)₂ was examined with an idealized octahedral coordination geometry around each W atom and a W–W distance of 2.20 Å. The expected MO expression of the quadruple bond is found. In Na[W₂(μ -OOCH)₂(OOCH)₄](H₂O), which was used as a model for **1**, the same qualitative bonding picture emerges despite the large geometrical distortion in coordination environment of each W atom. Of course, the degeneracy in the π orbitals is removed. The presence and orientation of the axial H₂O ligands affects the energies of the metal orbitals but does not affect their ordering. The Mulliken overlap populations between the metal centers is approximately independent of H₂O–W–W angle (1.39 and 1.41 for 156 and 180°, respectively), and it even decreases a small amount (to 1.24) when the axial ligands removed entirely. There is no obvious reason for a bond order lower than 3.5 to be found in the MO calculations. Certainly there are no dramatic effects such as are observed for bridged M₂L₁₀ systems.⁴¹

Concluding Remarks

Examples of the [Mo₂((μ -OOCR)₄(OOCR))⁻ ion are well-known, and even a [Mo₂((μ -OOCR)₄(OOCR)₂)²⁻ species has been discussed in terms of an intermediate in ligand exchange processes.^{42,43} The proposed structure of the latter is qualitatively different from that of **1**, and the latter offers another structural possibility for the intermediate. Alternatively, one can see in the structure of **1** the skeleton of the more highly oxidized W₃O₂(μ -OOCCH₃)₆(OOCCH₃)₂OH₂ complex (Figure

(32) McCarley, R. E.; Templeton, J. L.; Calburn, T. J.; Katovic, V.; Hoxmeier, R. J. *Adv. Chem. Ser.* **1975**, 150, 318.

(33) Santure, D. J.; Huffman, J. C.; Sattelberger, A. P. *Inorg. Chem.* **1985**, 24, 371.

(34) Hanaya, M.; Iwaizumi, M. *J. Organomet. Chem.* **1992**, 435, 337.

(35) Ball, J. M.; Boorman, P. M.; Moynihnan, K. J.; Patel, V. D.; Richardson, J. F.; Collison, D.; Mabbs, F. E. *J. Chem. Soc., Dalton Trans.* **1983**, 2479.

(36) Figgis, B. J.; Lewis, J. *Prog. Inorg. Chem.* **1964**, 6, 37.

(37) Cotton, F. A.; Wang, W. *Inorg. Chem.* **1984**, 23, 1604.

(38) Hopkins, M. D.; Gray, H. B.; Miskowski, V. M. *Polyhedron* **1987**, 6, 705.

(39) Chisholm, M. H.; Clark, D. L.; Huffman, C.; VanDerSluys, W. G.; Kober, E. M.; Lichtenberger, D. L.; Bursten, B. E. *J. Am. Chem. Soc.* **1987**, 109, 6796.

(40) Robin, M. B.; Day, P. *Adv. Inorg. Chem. Radiochem.* **1967**, 10, 248.

(41) Shaik, S.; Hoffmann, R.; Fiesel, C. R.; Summerville, R. H. *J. Am. Chem. Soc.* **1980**, 102, 4555.

(42) Cayton, R. H.; Chacon, S. T.; Chisholm, M. H.; Folting, K. *Polyhedron* **1993**, 12, 415.

(43) Teramoto, K.; Sasaki, Y.; Migita, K.; Iwaizumi, M.; Saito, K. *Bull. Chem. Soc. Jpn.* **1979**, 52, 446.

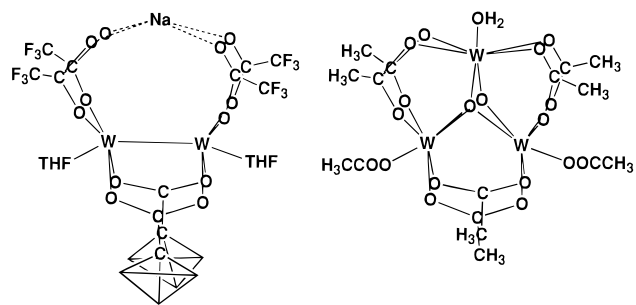


Figure 7. Comparison of the schematic structure of **1** with that of $W_3O_2(\mu\text{-OOCCH}_3)_6(\text{OOCCH}_3)_2\text{OH}_2$.

7).⁴⁴ That is, if two μ_3 -oxo groups and the H_2O ligand are removed, two $[\text{OOCCH}_3]^-$ ligands replaced with THF molecules, one W atom replaced with Na, and the W–W distance

(44) Bino, A.; Cotton, F. A.; Dori, Z.; Koch, S.; Kuppers, H.; Millar, M.; Sekutowski, J. C. *Inorg. Chem.* **1978**, *17*, 3245.

shortened from 2.75 to 2.45 Å, then one generates an analogue of **1**. Perhaps, then, **1** is better viewed as a model for an intermediate on the way to a $W_3O_2(\mu\text{-OOCR})_6(\text{OOCR}')_3$ complex. In contrast to other ligand systems where such species remain to be identified, the cluster substituents used here allow this putative intermediate to be isolated and characterized.

Acknowledgment. We are grateful to the National Science Foundation for research support and the Reilly Foundation for fellowship support (V.C.-P.). We thank Dr. G. P. A. Yap for the final report of structure **1** initiated by Dr. R. Ostrander. We also thank Prof. J. Furdyna for the use of the EPR facilities.

Supporting Information Available: Listings of X-ray parameters, anisotropic thermal parameters, complete atomic coordinates and displacement parameters, and complete bond lengths and angles and a drawing of the complete structure of **1** (13 pages). Ordering information is given on any current masthead page.

IC9609113